ISSN 1 746-7233, England, UK
World Journal of Modelling and Simulation
Vol. 11 (2015) No. 2, pp. 123-135

Modelling and optimal power control for permanent magnet synchronous generator wind turbine system connected to utility grid with fault conditions

Youssef Errami[1]*, Mohammed Ouassaid[2], Mohamed Maaroufi[3]

[1] Department of Physical, Faculty of Science, Chouaib Doukkali University, Eljadida, Morocco
[2] Department of Industrial Engineering, Ecole Nationale des Sciences Appliquées, Cadi Ayyad University, Safi, Morocco
[3] Department of Electrical Engineering Mohammadia School's of Engineers, Mohammed V- Agdal University, Rabat, Morocco

(*Received August 7 2013, Accepted March 13 2015*)

Abstract. This paper develops the model and the optimal power control strategy of maximizing wind energy tracking for Variable Speed Wind Energy Conversion System (VS-WECS) based Permanent Magnet Synchronous Generator (PMSG) and interconnected to the electric network. The VS-WECS model includes a Wind Turbine (WT), a PMSG, PWM rectifier in generator-side, intermediate DC circuit and PWM inverter in grid-side. Model of the proposed system in d-q axes reference frame is elaborated. The proposed strategy is based on a Vector Control (VC) approach for control of both PMSG and grid- side inverter of VS-WECS. The PMSG side rectifier control is used to keep the generator rotor velocity at an optimal value obtained from the Maximum Power Point Tracking (MPPT) algorithm to maximize the generated power from Wind Turbine Generator (WTG) under low, medium or high wind velocity mode. The grid-side inverter injects the generated power into the AC network, regulates DC-link voltage and it is used to achieve unity power factor. So, the proposed VC strategy is capable to fully decouple the quadrature (q) and direct (d) components of the currents. Moreover, a pitch control scheme is proposed to prevent wind turbine damage from excessive wind speed and to achieve power limitation. The performance of the proposed VC is evaluated with MATLAB/ Simulink environment in terms of MPPT, control of dc voltage, power limitation and power factor control. Simulation results reveal the achievability of the proposed control approach over the whole VS-WECS operating regions. The simulation results show that the proposed strategy has excellent performance for normal working conditions as well as for low voltage drop conditions.

Keywords: VS-WECS, PMSG, MPPT, Vector Control, variable-speed control, grid fault

1 Introduction

Over the last years, with technological advancement, wind turbine technology has grown rapidly and becomes the most competitive form of renewable energy sources[1, 2]. Besides, Variable Speed Wind Energy Conversion Systems (VS-WECS) with active control on the power output and turbine velocity can reduce stresses and load on various parts of the turbine structure, including the blades and tower. Consequently, longer life time, higher overall efficiency, and improved power quality make these VS-WECS economically competitive, despite their higher initial costs[3].

On the other hand, with the increased penetration of VS-WECS into power systems around the world, Wind Turbines Generators (WTGs) based on Permanent Magnet Synchronous Generator (PMSG) are becoming popular for variable-speed generation. PMSG offer several advantages such as: the elimination of a DC excitation system, no gearbox, full controllability of the system for Maximum Power Point Tracking (MPPT) control methodology to extract maximum power at different wind, high power density and high precision[4–6]. In addition, the development in power electronic devices has further played an important role in the perfection

* Corresponding author. *E-mail address*: errami.emi@gmail.com

of their controllability and reliability[6, 7]. So, the VS-WECS are at present required to participate actively in electric network operation by appropriate generation control methodologies[8].

In recent years, considerable research efforts have been done in the design of topologies and controllers for VS-WECS. Yi Wang et al.[9] have discussed power regulation of VS-WECS based PMSG during transient events to enhance the inertial response and damping ability of electrical network. Eduardo et al. and Jiekang et al.[10, 11] have proposed an adaptive control strategy for a VS-WECS based on a PMSG and a Pulse Width Modulated (PWM) current source converter. So, capacitor is required in this configuration and the generated reactive power as well as the voltage in the DC-link can be modified according to the wind speed. In multi megawatt WECS that necessitate a elevated dc-link voltage, June-Seok et al. and Yaramasu et al. and Jun et al.[12–14] have presented a multilevel Neutral Point Clamped (NPC) power converter to avoid the series connected to power electronics devices and because two-level topology is not appropriate due to the pricey switching devices with high specifications (current/ voltage) in high power wind systems. Direct control techniques for VS-WECS were proposed in [15–18]. They use hysteresis regulator and a switching lookup table to preserve estimations of the torque, the active and reactive power in some limits. The most important advantages of direct control approaches comprise rapid dynamic response, simple implementation and they do not necessitate rotary transformations. Marius et al.[19] investigate voltage harmonics compensation, the Ride Through Performance (RTP) of wind system during electrical network voltage sags, transition from stand alone to power grid connected and vice versa.

In this context, this study proposes a control scheme for VS-WECS based on the PMSG. The purpose of this work is to investigate system control to simultaneously provide MPPT, pitch control, regulates DC-link voltage and achieve unity power factor. Immunity against low voltage drop conditions caused by symmetrical Three-Line-to-Ground faults (3LG) is also provided in the proposed VS-WECS. The major contributions of this work can be summarized as follows:

(1) Maximum Power Point Tracking (MPPT) of the VS-WECS is realized in conjunction with the speed of PMSG to extract optimum power from the Wind Turbine (WT);
(2) Pitch Control algorithm is used to avoid overloading in case of high wind speed and to prevent wind turbine damage;
(3) Decoupling control strategy with Vector Control theory (VC) is applied to achieve MPPT, regulation of dc-link voltage, control of reactive and active power, and unity power factor under both variable and steady wind conditions;
(4) The control of the VS-WECS can tackle low voltage drop conditions caused by symmetrical Three-Line-to-Ground faults (3LG).

The remainder of this paper is organized as follows. In Section 2, the models of the wind turbine and PMSG are developed. In Section 3, Vector Control (VC) of the system will be presented. The simulations results are presented and analyzed in Section 4. Finally, some conclusions are given in Section 5.

2 Mathematical modelling of wind turbine generator

2.1 Model of wind turbine with PMSG

The mechanical power available from a variable speed wind turbine is expressed as [6]:

$$P_{\text{Turbine}} = \frac{1}{2}\rho A C_P(\lambda, \beta) v^3, \tag{1}$$

where, ρ is the air density (typically 1.225 kg/m^3), A is the area swept by the rotor blades (in m^2), C_p is the coefficient of power conversion and ν is the wind speed (in m/s). The tip-speed ratio λ is given by

$$\lambda = \frac{\omega_m R}{v}, \tag{2}$$

where ω_m and R are the rotor angular velocity (in rad/sec) and rotor radium (in m), respectively. The wind turbine mechanical torque output T_m is given as:

$$T_m = \frac{1}{2}\rho A C_P(\lambda,\beta)v^3\frac{1}{\omega_m}. \tag{3}$$

The power coefficient is a nonlinear function of the tip-speed ratio λ and the blade pitch angle β (in degrees). If the swept area of the blade and the air density are constant, the value of C_p is a function of λ, and it is maximum at the particular λ_{opt}[20]. Then:

$$P_{\text{Turbine}} = \frac{1}{2}\rho A C_{P\max} v^3, \tag{4}$$

A generic equation is used so as to model the power coefficient $C_p(\lambda,\beta)$ based on the modelling turbine characteristics described in [21] as:

$$\begin{aligned} C_P &= \frac{1}{2}\left(\frac{116}{\lambda_i} - 0.4\beta - 5\right)e^{-\left(\frac{21}{\lambda_i}\right)}, \\ \frac{1}{\lambda_i} &= \frac{1}{\lambda + 0.08\beta} - \frac{0.035}{\beta^3 + 1}. \end{aligned} \tag{5}$$

The maximum value of C_p, that is $C_{p\max}$, is achieved for $\beta = 0$ and for $\lambda_{opt} = 8.1$. Hence, to fully utilize the wind energy, λ should be maintained at λ_{opt}, which is determined from the blade design. The particular value λ_{opt} results in the point of optimal efficiency where the maximum power is captured from wind by the wind turbine generator. So, for each wind speed, there exists a specific point in the wind turbine power characteristic, MPPT, where the output power is maximized. Thus, the control of the wind farm load results in a variable-speed operation of the turbine generator. Then, the maximum power is extracted continuously from the wind (MPPT control) [22]. That is illustrated in Fig. 1.

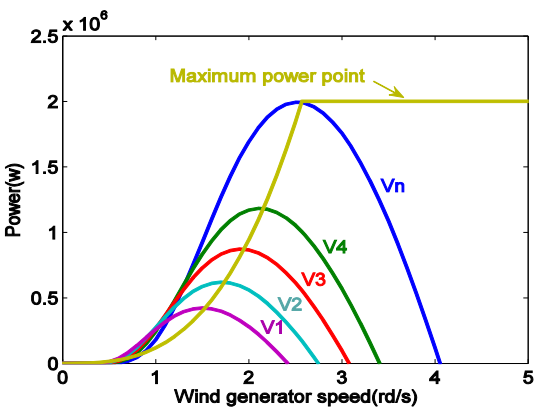

Fig. 1. Wind generator power curves at various wind speed

2.2 PMSG modelling

Dynamic modelling of PMSG can be described in $d-q$ reference system as follows [22]:

$$v_{gq} = (R_g + p.L_q)\,.i_q + \omega_e L_d i_d + \omega_e \psi_f, \tag{6}$$

$$v_{gd} = (R_g + pL_d)\,i_d - \omega_e L_q i_q, \tag{7}$$

where v_{gd} and v_{gq} are the direct stator and quadrature stator voltage, respectively. i_d and i_q are the direct stator and quadrature stator current, respectively. R_g is the stator resistance, L_q and L_q are the inductances of the generator on the d and q axis, ψ_f is the permanent magnetic flux and ω_e is the electrical rotating speed of the generator, defined by

$$\omega_e = p_n \omega_m, \tag{8}$$

where ω_m is the mechanical angular speed and p_n is the number of pole pairs of the generator. The expression for the electromagnetic torque can be described as:

$$T_e = \frac{3}{2} p_n \left[\psi_f i_q - (L_d - L_q)\, i_d i_q\right]. \tag{9}$$

The dynamic equation of the wind turbine is described by:

$$J\frac{d\omega_m}{dt} = T_e - T_m - F\omega_m, \tag{10}$$

where J is the moment of inertia, F is the viscous friction coefficient and T_m is the mechanical torque developed by the turbine .

3 Control strategy of the VS-WECS

3.1 Adopted MPPT control algorithm

For a given wind speed, the optimal rotational speed of the wind turbine rotor, from (2), can be estimated as follows[23]:

$$\omega_{m-opt} = \frac{v\lambda_{opt}}{R}. \tag{11}$$

Each wind turbine can produce maximum power by (4). Thus, the maximum mechanical output power of the turbine is given as follows:

$$P_{\text{Turbine\_max}} = \frac{1}{2}\rho A C_{P\max}\left(\frac{R\omega_{m-opt}}{\lambda_{opt}}\right)^3. \tag{12}$$

Then, we can get the maximum power $P_{\text{Turbine\_max}}$ by regulating the turbine speed in different wind speed under rated power of the wind power system. So, an optimum value of tip speed ratio λ_{opt} can be maintained and maximum wind power can be captured. The P_{MPPT} curve is defined as function of ω_{m-opt}, the speed referred to the generator side:

$$P_{MPPT} = K\omega_{m-opt}^3. \tag{13}$$

So as to regulate the aerodynamic power extracted from the wind, the power control is used at high wind speed. Then, when the wind speed reached the nominal value, the pitch angle controller enters in operation in order to decrease the power coefficient. For each wind turbine, the simplified representation of wind turbine control diagram is shown in Fig. 2 where P_{gp} is the generated power. Then, when the power output becomes too high the blade pitch is asked to immediately turn the blades slightly out of the wind. So, the rated rotor speed and the power are maintained for above rated wind speed[24].

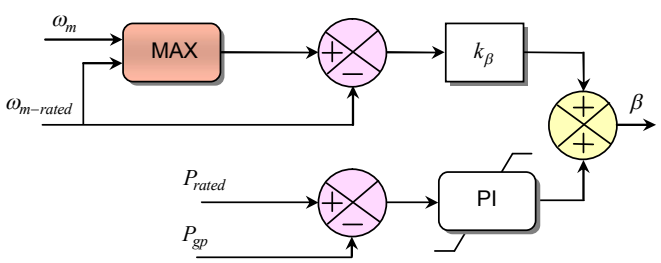

Fig. 2. WECS Pitch angle controller

3.2 Control strategy of the generator side converter with vector control and MPPT

The PMSG side converter is used as a rectifier and works as a driver to control the generator operating at optimum rotor speed ω_{m_opt}. On the other hand, it is deduced from Eqs. (9) and (10) that the generator velocity can be controlled by regulating the q-axis stator current components (i_{qr}). Consequently, Vector Control (VC) is used with optimal rotor velocity ω_{m-opt} to obtain MPPT for any particular wind speed. The control scheme shown in Fig. 3 is used as the control methodology for the PMSG side rectifier. So, double closed loop regulate is used. Also, u_{sq} is obtained by the error of i_{qr} and i_q where i_{qr} is the reference current. This error is delivered to a PI controller. In order to reduce the copper loss, the d-axis current component i_{dr} is set to zero. Moreover, voltage feed forward compensations, Δu_{sq} and Δu_{sd} are added into the control block so as to improve the dynamic response. Finally, we use PWM to produce the control signal to implement the vector control for the PMSG.

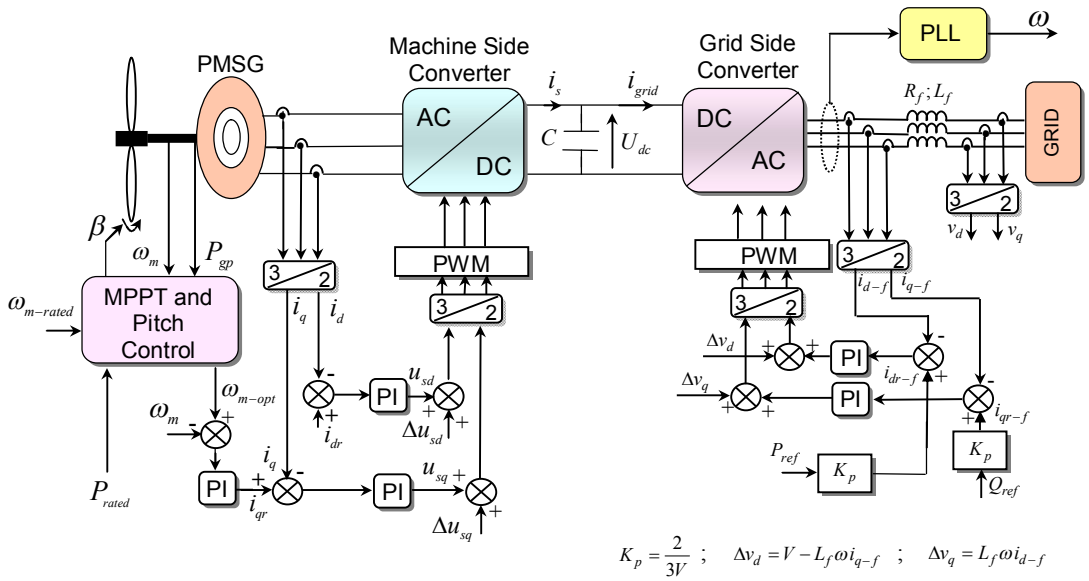

Fig. 3. Schematic of control strategy for VS-WECS based on the PMSG

3.3 Grid-side controller methodology and implementation

The grid side converter is used to deliver the energy from the PMSG side to the grid, to regulate the DC bus voltage and to adjust the quantity of the reactive and active powers delivered to the grid during wind variation in order to achieve Unity Power Factor (UPF) for any wind speed. As a result, the Vector Control with PI control loops is employed. The controller is shown in Fig. 3. Then, in the inner control loops, PI controllers are used to regulate direct and quadrature current components, respectively, while, in the second loop, the DC-voltage PI controller stabilize the DC voltage to the reference value. Furthermore, the decoupling voltages are added to the current controller outputs to compensate the cross-coupling effect due to the output filter in the rotating synchronously reference frame.

According to Fig. 3, the relationship between the line currents and the grid inverter voltages is given by:

$$\begin{bmatrix} e_a \\ e_b \\ e_c \end{bmatrix} = R_f \begin{bmatrix} i_a \\ i_b \\ i_c \end{bmatrix} + L_f \frac{d}{dt} \begin{bmatrix} i_a \\ i_b \\ i_c \end{bmatrix} + \begin{bmatrix} v_a \\ v_b \\ v_c \end{bmatrix}, \tag{14}$$

where:

e_a, e_b, e_c	voltages at the inverter system output;
v_a, v_b, v_c	grid voltage components;
i_a, i_b, i_c	line currents;
L_f	filter inductance;
R_f	filter resistance.

Transferring Eq. (14) in the reference frame rotating synchronously with the electrical grid voltage vector, the model for the grid-side converter is given by [25]:

$$v_q = e_q - R_f i_{q-f} - L_f \frac{di_{q-f}}{dt} - \omega L_f i_{d-f}, \tag{15}$$

$$v_d = e_d - R_f i_{d-f} - L_f \frac{di_{d-f}}{dt} + \omega L_f i_{q-f}, \tag{16}$$

where:

e_d, e_q	inverter d-axis and q-axis voltage components;
v_d, v_q	grid voltage components in the d-axis and q-axis;
i_{d-f}, i_{q-f}	d- axis current and q- axis current of grid.
ω	network angular frequency

The VC scheme used is based on a rotating reference frame as shown in Fig. 4. The instantaneous powers are given by [21]:

$$Q = \frac{3}{2}(v_d i_{q-f} - v_q i_{d-f}), \tag{17}$$

$$P = \frac{3}{2}(v_d i_{d-f} + v_q i_{q-f}). \tag{18}$$

The DC-side equation can be given by (Fig. 3):

$$C\frac{dU_{dc}}{dt} = i_s - i_{grid}, \tag{19}$$

where:

U_{ab}	dc-link voltage;
i_s	PMSG side current
i_{grid}	grid side transmission line current;
C	dc-link capacitor.

So, we can rewrite Eq. (19) as:

$$C\frac{dU_{dc}}{dt} = \frac{P_{gp}}{U_{dc}} - i_{grid}. \tag{20}$$

The Vector Control scheme used is based on a rotating synchronously reference frame as shown in Fig. 4. Then:

$$\begin{aligned} v_d &= V, \\ v_q &= 0. \end{aligned} \tag{21}$$

Thus, Eqs. (15-16) may be expressed as:

$$L_f \frac{di_{d-f}}{dt} = e_d - R_f i_{d-f} + \omega L_f i_{q-f} - V, \tag{22}$$

$$L_f \frac{di_{q-f}}{dt} = e_q - R_f i_{q-f} - \omega L_f i_{d-f}. \tag{23}$$

Then, using (17) and (18), the reactive power and active power can be expressed as:

$$P = \frac{3}{2} V i_{d-f}, \tag{24}$$

$$Q = \frac{3}{2} V i_{q-f}. \tag{25}$$

As a result, reactive and active power control can be controlled by quadrature and direct current components, respectively. Then

$$i_{qr-f} = \frac{2}{3V} Q_{ref}, \tag{26}$$

$$i_{dr-f} = \frac{2}{3V} P_{ref}, \tag{27}$$

where i_{qr-f} and i_{dr-f} are the reference signal of q-axis and d-axis current, respectively. Q_{ref} and P_{ref} are the reference of reactive and active power, respectively. Moreover, the inverter is used to transfer all the active power produced by the WTG to the utility grid and also to produce no reactive power so that UPF is obtained. Consequently, the DC-link voltage must remain constant[26]. The control methodology for grid side inverter is shown in Fig. 3. It is fundamental to use two closed-loop controls to regulate the DC bus voltage and the required transmission line current. Fig. 5 shows de control scheme of DC-bus voltage where P_{gp} is the active power delivered from the PMSG.

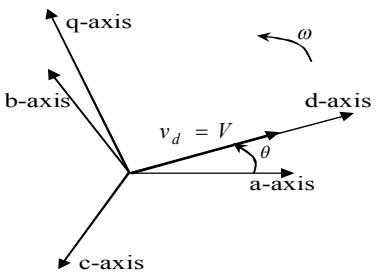

Fig. 4. Abc and rotating reference frame

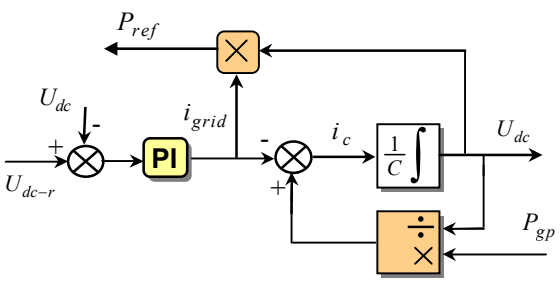

Fig. 5. Control of DC-bus voltage

Also, the fast dynamic is associated with the line current control in the inner loop where the Vector control is used to track the line current control (Fig. 3). In the outer loop, slow dynamic is associated with the DC voltage control (Fig. 5). The d-axis reference current is determined by DC-bus voltage controller in order to control the converter output real power. For this reason, we use the PI regulator to generate the reference source current i_{dr-f} and regulate the DC voltage. Although the reference signal of the q-axis current i_{qr-f} is produced by the reactive power Q_{ref} according to (26). To compensate the cross-coupling effect due to the output filter in the rotating synchronously reference frame, the decoupling voltages are added to the current controller outputs. For that reason, we use: e'_d et e'_q as:

$$R_f i_{d-f} + L_f \frac{di_{d-f}}{dt} = e'_d, \tag{28}$$

$$R_f i_{q-f} + L_f \frac{di_{q-f}}{dt} = e'_q. \tag{29}$$

Then, the inverter q-axis d-axis voltage components can be given by:

$$e_d = e'_d - L_f \omega i_{q-f} + V, \tag{30}$$

$$e_q = e'_q + L_f \omega i_{d-f}. \tag{31}$$

Consequently, e'_d and e'_q are calculated as follows:

$$e'_d = K_P(i_{dr-f} - i_{d-f}) + K_I \int (i_{dr-f} - i_{d-f})dt, \tag{32}$$

$$e'_q = K_P(i_{qr-f} - i_{q-f}) + K_I \int (i_{qr-f} - i_{q-f})dt. \tag{33}$$

Fig. 3 shows the control block diagram of grid-side PWM inverter based on the above strategy. There are two closed-loop controls and PWM is used so as to produce the control signal to control the grid-side converter. Also, the decoupling voltages, Δv_q et Δv_d, are added to the current controller outputs to compensate the cross-coupling effect.

4 Simulation results

The complete VS-WECS with PMSG was simulated by Matlab/Simulink using the parameters given in Tab. 1. During the simulation, for the PMSG side converter control system, the d axis command current, i_{dr} is set to zero. For the grid side inverter, Q_{ref} is set to zero. The DC-link voltage reference is fixed at $U_{dc-r} = 1500V$ and the electric grid frequency value is steady at 50 Hz. The topology of the studied VS-WECS based on PMSG connected distribution network is depicted in Fig. 6. The grid voltage phase lock loop (PLL) is implemented.

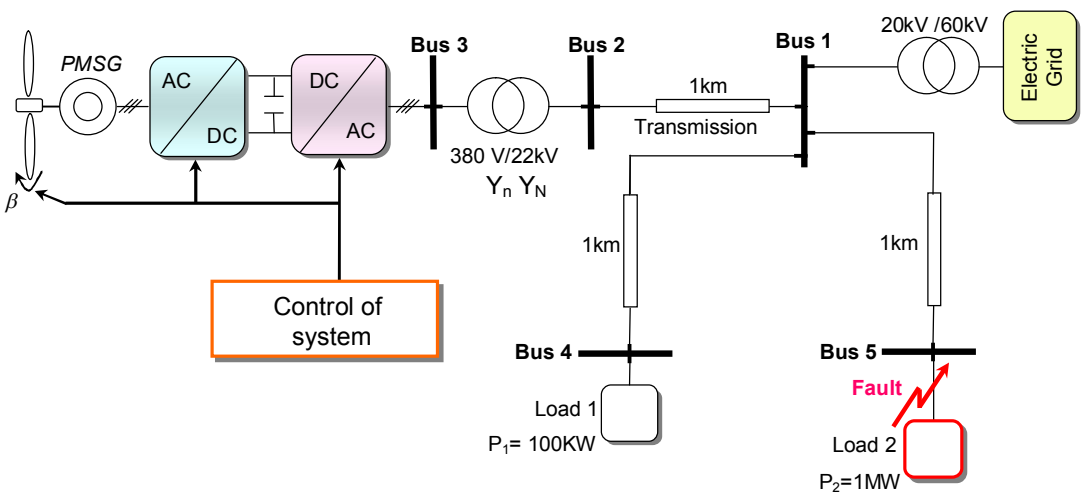

Fig. 6. Configuration of the system

4.1 Normal working conditions

Fig. 7 illustrates the profile of wind velocity and rated wind speed considered in the simulation ($v_n = 12.4\ m/s$). Fig. 8 to Fig. 11 show the simulation results of pitch angle, coefficient of power conversion C_p, power generated and rotor angular velocity for VS-WECS. It can be seen that, if the wind velocity increases, then rotor angular speed of PMSG increases proportionally too, with a limitation. This velocity limit will be obtained by the pitch angle variations. When the system operates under MPPT control strategy, the performance coefficient C_p is maintained to its maximum value ($C_{P\max} = 0.41$) and the pitch angle is $\beta = 0°$. But, if the wind velocity reaches the rated wind speed of the turbine ($v_n = 12.4$ m/s), C_p is decreasing

because the operation of the pitch angle control is actuated and β increases. So, rotational speed and power generated are keeping constants. The rotational speed of turbine is effectively limited to 2.57 rd/s. In addition, generated power is optimized with MPPT strategy and keeps at his nominal value when the wind speed exceeds the nominal value. Consequently, the limitation of the power captured and so of the turbine velocity is carried out using the pitch control. Fig. 11 illustrates the waveforms of the optimum velocity and the velocity of PMSG. It is seen that the PMSG speed follows the reference speed very closely. Fig. 14 and Fig. 15 show the variation and a closer observation of three phase voltage and current at Bus 3 (Fig. 6). The frequency imposed by the grid is 50 Hz. we see that unity power factor is achieved approximatively. Fig. 12 shows the simulation result of DC link voltage that remains a constant value. Therefore, this proves the effectiveness of the established regulators.

4.2 Fault working conditions

The fault event is a three-phase to ground short-circuit fault, at the Bus 5 of the 1 MW loads, is introduced at $t = 3\ s$ for 150 ms. As illustrated in Fig. 13 and Fig. 14, a three-phase grid short circuit fault at 3 s forces the grid voltage to drop from 100% to 4% of its nominal values and the voltage dip lasts for 150 ms as it is shown in Fig. 14. Fig. 13 illustrates the waveform of RMS lines ground voltages at Bus 3 during the grid fault period.

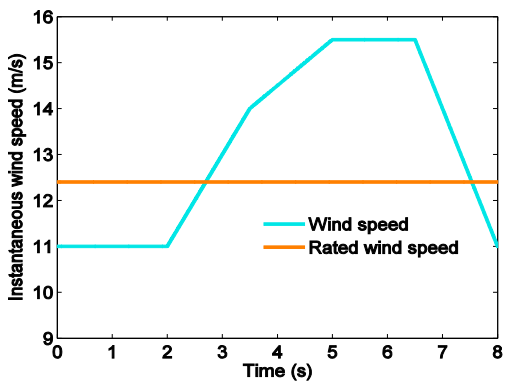

Fig. 7. Instantaneous wind speed (m/s)

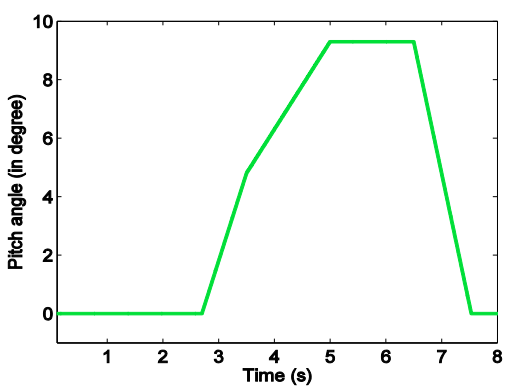

Fig. 8. Pitch angle (in degree)

Fig. 14 and Fig. 15 show the variation and a closer observation of three phase voltage and current of three phase voltage at Bus 3. It can be seen that, after faults removed, the grid voltage recovers and the three voltages take their initial values. It is obvious from Fig. 12 that the DC link voltage remains a constant value

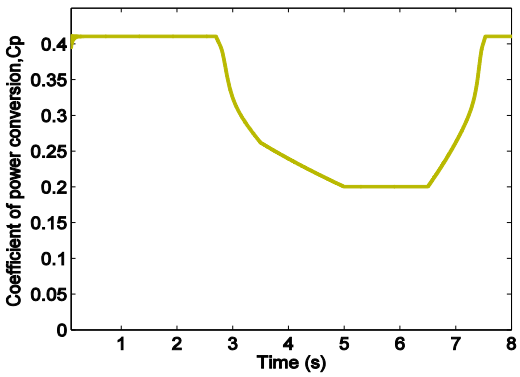

Fig. 9. Coefficient of power conversion

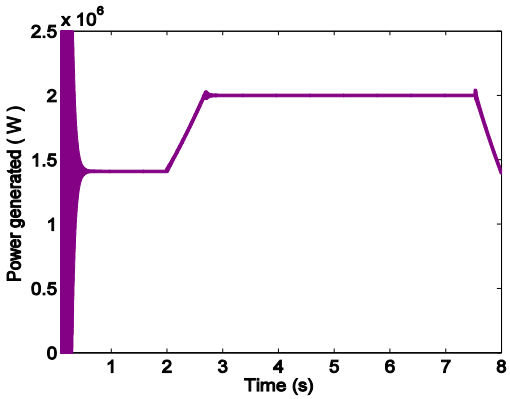

Fig. 10. Generated power (W)

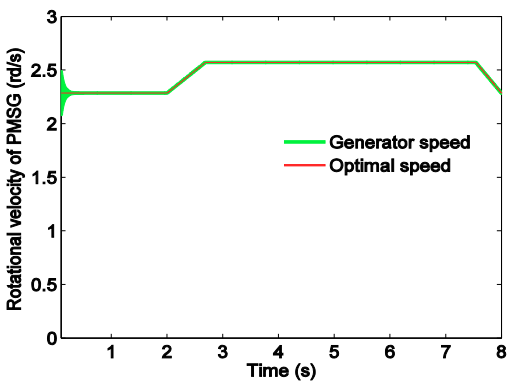

Fig. 11. Speed of PMSG (rd/s)

and the three phase voltage variations will not be transferred to the DC link voltage. So, the DC link voltage has been controlled to enhance dynamic performance of the VS-WECS.

5 Conclusion

This work has successfully designed a VC to control a VS-WECS based on the PMSG and connected to the electrical network. The control methodology is applied for inverter and for generator converter. The efficiency of the proposed VC scheme is confirmed by simulations with different examined cases of wind speed and state of the power grid. The simulations highlighted that the proposed control strategy posses excellent performance under changing operating conditions. The major contributions of this work can be summarized as follows:

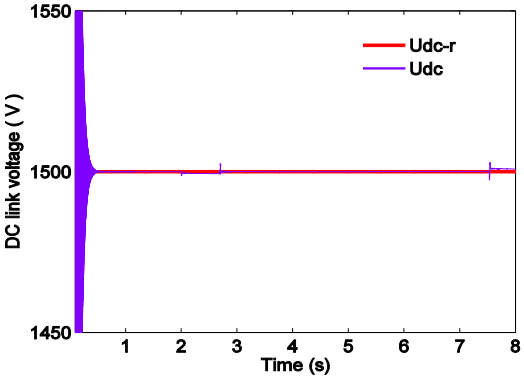

Fig. 12. DC link voltage (V)

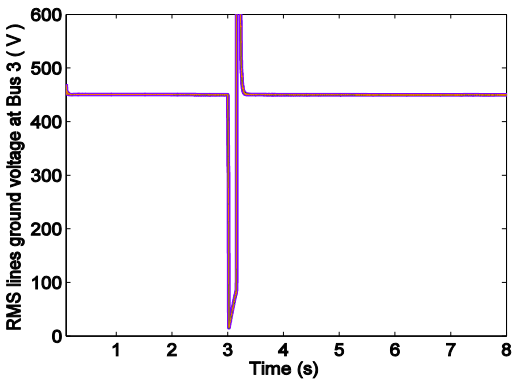

Fig. 13. RMS lines ground voltages at Bus 3 (V)

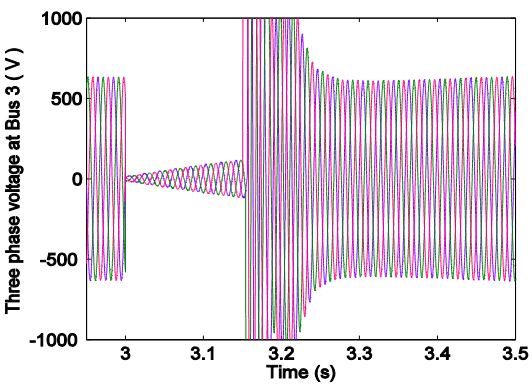

Fig. 14. Three phase voltage at Bus 3

(1) The successful construction of the mathematical model of a VS-WECS based PMSG and interconnected to the power grid.

(2) The successful utilisation of a VC approach as the major control scheme based on PI controllers to improve the VS-WECS functioning performance, with the objectives of MPPT, regulation of dc-link voltage, control of reactive and active power, and unity power factor under both variable and steady wind conditions.

(3) Pitch angle controller to prevent wind turbine damage from excessive wind speed.

(4) The method presents a very high immunity against low voltage drop conditions caused by symmetrical Three-Line-to-Ground faults (3LG).

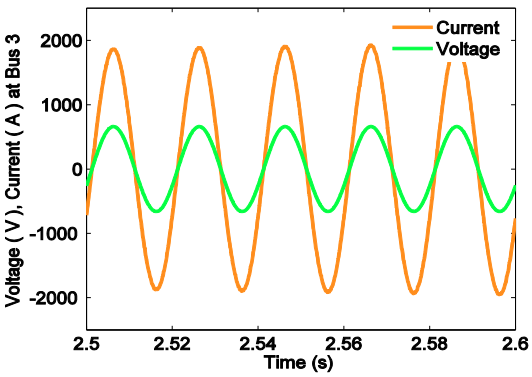

Fig. 15. The waveforms of three Phase current and voltage at Bus 3

Appendix

Table 1. Please write your table caption here

Parameter	Value
P_r rated power	2 (Mw)
ω_m rated mechanical speed	2.57 (rd/s)
R stator resistance	0.008(Ω)
L_d stator d-axis inductance	0.0003 (H)
L_q stator q-axis inductance	0.0003 (H)
ψ_f permanent magnet flux	3.86 (wb)
p_n pole pairs	60

References

[1] F. Luo, K. Meng, et al. Coordinated operational planning for wind farm with battery energy storage system. *IEEE Transactions On Sustainable Energy*, 2015, **6**(1): 253–262.

[2] F. Bu, Y. Hu, et al. Wide-speed-range-pperation dDual stator-winding induction generator DC generating system for wind power applications. *IEEE Transactions On Power Electronics*, 2015, **30**(2): 561–573.

[3] D. Melo, L. Chang-Chien. Synergistic control between hydrogen storage system and offshore wind farm for grid operation. *IEEE Transactions on Sustainable Energy, January*, 2014, **5**(1): 18–27.

[4] S. Alshibani, V. Agelidis, R. Dutta. Lifetime cost assessment of permanent magnet synchronous generators for MW level wind turbines. *IEEE Transactions on Sustainable Energy*, 2014, **5**(1): 10–17.

[5] B.Aubert, J. Régnier, et al. Kalman-Filter-based indicator for online interturn short circuits detection in permanent-magnet synchronous generators. *IEEE Transactions on Industrial Electronics*, 2015, **62**(3): 1921–1930.

[6] I. Jlassi, J. Estima, et al. Multiple open-circuit faults diagnosis in back-to-back converters of PMSG drives for wind turbine systems. *IEEE Transactions on Power Electronics*, 2015, **30**(5): 2689–2702.

[7] F. Blaabjerg, K. Ma. Future on power electronics for wind turbine systems. *IEEE Journal of Emerging And Selected Topics in Power Electronics*, 2013, **1**(3): 139–152.

[8] S. Alepuz, A. Calle, et al. Use of stored energy in PMSG rotor inertia for low-voltage ride-through in back-to-back NPC converter-based wind power systems. *IEEE Transactions on Industrial Electronics*, 2013, **60**(5): 1787–1796.

[9] Y. Wang, J. Meng, et al. Control of PMSG-based wind turbines for system tnertial response and power oscillation damping. *IEEE Transactions on Sustainable Energy*, 2015, (99) DOI:10.1109/TSTE.2015.2394363.

[10] E. Giraldo, A. Garces, An adaptive control strategy for a wind energy conversion system based on PWM-CSC and PMSG. *IEEE Transactions on Power Systems*, 2014, **29**(3): 1446–1453.

[11] W. Jiekang, J. Cheng, et al. Adaptive PI algorithm of SSSC controller for power flow of power systems based on neural networks. **in:** *Proceeding of Asia-Pacific Power and Energy Engineering Conference (APPEEC 2009)*, 2009, pp. 1–4.

[12] J. Lee, K. Lee. Open-switch fault tolerance control for a three-level NPC/T-type rectifier in wind turbine. *IEEE Transactions on Industrial Electronics*, 2015, **62**(2): 1012–1021.

[13] V. Yaramasu, W. Bin, et al. Predictive control for low-voltage ride-through enhancement of three-level-boost and NPC-converter-based PMSG wind turbine. *IEEE Transactions on Industrial Electronics*, 2014, **1**(12): 832–6843.

[14] L. Jun, S. Bhattacharya, A. Huang. A new nine-level active NPC (ANPC) converter for grid connection of large wind turbines for distributed generation. *IEEE Transactions on Power Electronics*, 2011, **26**(3): 961–972.

[15] M. Nuno, A. Freire, J. Cardoso. A fault-tolerant direct controlled PMSG drive for wind energy conversion systems. *IEEE Transactions on Industrial Electronics*, 2014, **61**(2): 821–834.

[16] Z.Zhang, Y. Zhao, et al. A space-vector-modulated sensorless direct-torque control for direct-drive PMSG wind turbines. *IEEE Transactions on Industry Applications*, 2014, **50**(4): 2331–2341.

[17] A. Harrouz, A. Benatiallah, O. Harrouz. Direct power control of a PMSG dedicated to standalone wind energy systems. *IEEE Eighth International Conference and Exhibition on Ecological Vehicles and Renewable Energies (EVER)*, 2013, pp. 1–5.

[18] A. Rajaei, M. Mohamadian, A. Varjani. Vienna-rectifier-based direct torque control of PMSG for wind energy application. *IEEE Transactions on Industrial Electronics*, 2013, **60**(7): 2919–2929.

[19] M. Fatu, F. Blaabjerg, I. Boldea. Grid to standalone transition motion-sensorless dual-inverter control of PMSG with asymmetrical grid voltage sags and harmonics filtering. *IEEE Transactions on Power Electronics*, 2014, **29**(7): 3463–3472.

[20] C. Huang, F. Li, et al. Second-order cone programming-based optimal control strategy for wind energy conversion systems over complete operating regions. *IEEE Transactions on Sustainable Energy*, 2015, **6**(1): 263–271.

[21] Y. Errami, M. Hilal, et al. Nonlinear control of MPPT and grid connected for variable speed wind energy conversion system based on the PMSG. *Journal of Theoretical and Applied Information Technology*, 2012, **39**(2): 205–217.

[22] F. Bu, Y. Hu, et al. Wide-speed-range-operation dual stator-winding onduction generator DC generating system for wind power applications. *IEEE Transactions on Power Electronics*, 2015, **30**(2): 561–573.

[23] J. Yan, H. Lin, et al. Improved sliding mode model reference adaptive system speed observer for fuzzy control of direct-drive permanent magnet synchronous generator wind power generation system. *IET Renewable Power Generation*, 2013, **7**(1): 28–35.

[24] Y. Errami, M. Maaroufi, M. Ouassaid. Maximum power point tracking of a wind power system based on the PMSG using sliding mode direct torque control. **in:** *Renewable and Sustainable Energy Conference (IRSEC), 2013 International*, 2013, pp.218–223, doi: 10.1109/IRSEC.2013.6529706

[25] H. Shariatpanah, R. Fadaeinedjad, M. Rashidinejad. A new model for PMSG-based wind turbine with yaw control. *IEEE Transactions on Energy Conversion*, 2013, **28**(4): 929–937.

[26] Y. Errami, M. Ouassaid, M. Maaroufi. Variable structure control for permanent magnet synchronous generator based wind energy conversion system operating under different grid conditions. **i**n:*Complex Systems (WCCS) 2014 Second World Conference*, 2014, **1**: 340–345, doi: 10.1109/ICoCS.2014.7060996.